Microscopic Features of Bosonic Quantum Transport and Entropy Production

Mihail Mintchev,* Luca Santoni, and Paul Sorba

The microscopic features of bosonic quantum transport in a nonequilibrium steady state, which breaks time reversal invariance spontaneously, are investigated. The analysis is based on the probability distributions, generated by the correlation functions of the particle current and the entropy production operator. The general approach is applied to an exactly solvable model with a point-like interaction driving the system away from equilibrium. The quantum fluctuations of the particle current and the entropy production are explicitly evaluated in the zero frequency limit. It is shown that all moments of the entropy production distribution are non-negative, which provides a microscopic version of the second law of thermodynamics. On this basis a concept of efficiency, taking into account all quantum fluctuations, is proposed and analyzed. The role of the quantum statistics in this context is also discussed.

1. Introduction

This paper focuses on the basic microscopic properties of the particle and heat transport and the relative entropy production in nonequilibrium bosonic quantum systems of the type shown in **Figure 1**. The bulk of the system consists of two semi-infinite leads L_i, which are attached at infinity to two heat reservoirs (baths) R_i. The latter are both sources and sinks of particles and have large enough capacities, so that the particle emission and absorption do not change the (inverse) temperature $\beta_i \geq 0$ and the chemical potential μ_i of R_i. The contact between the two leads at $x = 0$ represents a point-like impurity described by a unitary scattering matrix $\mathbb{S}$.

The bosonic junction, shown schematically in Figure 1, can be engineered by using ultracold Bose gases,[1–3] which attract

Prof. M. Mintchev
Istituto Nazionale di Fisica Nucleare and Dipartimento di Fisica
Largo Pontecorvo 3, 56127 Pisa, Italy
E-mail: mintchev@df.unipi.it

Dr. L. Santoni
Institute for Theoretical Physics and Center for Extreme Matter and
Emergent Phenomena
Utrecht University
Leuvenlaan 4, 3584 CE Utrecht, The Netherlands

Prof. P. Sorba
LAPTh, Laboratoire d'Annecy-le-Vieux de Physique Théorique, Centre
National de la Recherche Scientifique
Université de Savoie
BP 110, 74941 Annecy-le-Vieux, France

recently much experimental and theoretical attention. The remarkable control over the interactions and the geometry of the samples in such experiments, as well as the absence of uncontrolled disorder, allow to explore unique aspects of many-body quantum physics. The advance in this rapidly developing area opens new horizons, including the possibility to create[4–6] bosonic analogues of the conventional mesoscopic electronic devises like diodes and transistors (atomtronics).

Coming back to the system in Figure 1, one can imagine that the reservoirs R_i contain ultracold atoms and are connected by two 1D traps, which are implemented by confining electromagnetic fields and form the leads. The contact point between the two traps realizes the impurity represented at the theoretical level by the scattering matrix $\mathbb{S}$. If the associated transmission probability $|\mathbb{S}_{12}|^2$ does not vanish, the system is away from equilibrium provided that the temperatures and/or chemical potentials of the two heat baths are different.

The departure from equilibrium gives origin of incoming and outgoing matter and energy flows from the reservoirs R_i. Some decades ago Landauer[7] and later Büttiker[8] proposed an efficient method for studying these flows. The Landauer–Büttiker (LB) approach is based on the scattering matrix $\mathbb{S}$ and goes beyond the linear response approximation, thus representing an essential tool of modern quantum transport theory. The LB framework has been further generalized in refs. [9–11] and finds nowadays various applications, ranging from the computation of the noise power[12–19] to the full counting statistics.[20–27] Most of the quoted studies have been performed for fermionic systems. Triggered by the growing experimental activity with ultracold Bose cases, the investigation below is devoted to the bosonic case. In the Section 2 we propose a general and universal approach to quantum transport at the microscopic level. In Sections 3– 5 we illustrate this approach at work, studying in detail an exactly solvable model. The role of the statistics is discussed in Section 6. Finally, Section 7 collects our conclusions and ideas for future investigations on the subject.

2. General Framework and Strategy

The basic observables, which characterize the quantum transport in the junction, are the particle current $j(t, x, i)$ flowing in the

**ADVANCED
SCIENCE NEWS**

www.advancedsciencenews.com
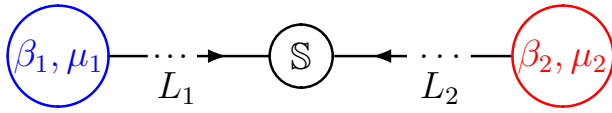
**annalen
der physik**

www.ann-phys.org

Figure 1. Two-terminal junction with bosonic heath baths connected with 1D traps and a contact defect.

lead L_i and the entropy production $\dot{S}(t, x)$ in the whole system. They provide local and global information, respectively, concerning the transport and its irreversibility. This information is codified in the correlation functions

$$w_n[j_i](t_1, x_1, \ldots, t_n, x_n) = \langle j(t_1, x_1, i) \cdots j(t_n, x_n, i)\rangle_{\mathrm{LB}} \quad (1)$$

and

$$w_n[\dot{S}](t_1, x_1, \ldots, t_n, x_n) = \langle \dot{S}(t_1, x_1) \cdots \dot{S}(t_n, x_n)\rangle_{\mathrm{LB}} \quad (2)$$

where the expectation value $\langle \cdots \rangle_{\mathrm{LB}}$ is computed in the LB state.[28] Following the standard approach[18–27] to full counting statistics, it is instructive to investigate the zero-frequency limits $\mathcal{W}_n[j_i]$ of $w_n[j_i]$ and $\mathcal{W}_n[\dot{S}]$ of $w_n[\dot{S}]$, integrating the quantum fluctuations over long periods of time. In this limit, the dependence on the $2n$ space–time variables in (1) and (2) drops out and one arrives at the following integral representations

$$\mathcal{W}_n[j_i] = \int_0^\infty \frac{\mathrm{d}\omega}{2\pi} \mathcal{M}_n[j_i](\omega) \quad (3)$$

$$\mathcal{W}_n[\dot{S}] = \int_0^\infty \frac{\mathrm{d}\omega}{2\pi} \mathcal{M}_n[\dot{S}](\omega) \quad (4)$$

Here ω is the energy and $\mathcal{M}_n[j_i]$ and $\mathcal{M}_n[\dot{S}]$ are the *moments* of two probability distributions $\varrho[j_i](\omega)$ and $\varrho[\dot{S}](\omega)$, which govern the quantum fluctuations of the particle current and the entropy production, respectively. The derivation of these distributions is a fundamental point of our approach. In fact, it turns out that $\varrho[j_i]$ and $\varrho[\dot{S}]$ control, respectively, the elementary processes of emission and absorption of particles from the reservoirs and the associated entropy production. More precisely, $\varrho[j_i]$ provides the quantum probabilities $\{p_k(\omega) : k = 0, \pm 1, \pm 2, \ldots\}$ for the aforementioned processes, whereas $\varrho[\dot{S}]$ gives the values $\{\sigma_k(\omega) : k = 0, \pm 1, \pm 2, \ldots\}$ of the associated entropy production.

In order to illustrate the above concepts at work, we propose and analyze in the paper an exactly solvable model. In this case, we derive $p_k(\omega)$ and $\sigma_k(\omega)$ and show that they fully characterize the quantum transport and its efficiency at the *microscopic level*. A fundamental achievement of the paper is the explicit form of the probabilities $p_k(\omega)$ in terms of the Bose distributions $d_i(\omega)$ of the heat reservoirs R_i.

The results about $\varrho[j_i]$ and $\varrho[\dot{S}]$ shed new light on various central aspects of nonequilibrium quantum systems. First of all, they clarify the deep role of the statistics. The analysis in ref. [27] demonstrated that for fermions the Pauli exclusion principle implies $p_k(\omega) = 0$ for all k different from 0 and ± 1. We show below that this is not the case for bosons, where $p_k(\omega) \neq 0$ for all $k = 0, \pm 1, \pm 2, \ldots$. This feature is the microscopic origin of the different quantum transport properties of fermionic and bosonic systems.

Another key aspect of our investigation concerns a remarkable feature of the entropy production distribution $\varrho[\dot{S}]$. We prove below that all moments of this distribution are non-negative

$$\mathcal{M}_n[\dot{S}](\omega) \geq 0, \qquad \forall\, n = 1, 2, \ldots \quad (5)$$

The bound (5) extends to the bosonic case our previous result[30] for fermions and can be interpreted as a quantum counterpart of the second law of thermodynamics for the nonequilibrium bosonic system in Figure 1. On this ground we propose an analog ε_{II} of the concept of second law efficiency[31] from macroscopic thermodynamics. The knowledge of the distribution $\varrho[\dot{S}]$ allows to separate at the fundamental level the processes with positive and negative entropy production and to extract from this information the coefficient ε_{II}, which takes into account the quantum fluctuations and characterizes in an intrinsic way the transport in the system.

In this paper we consider systems where the particle number and the total energy are conserved. These symmetries imply the existence of a conserved particle current $j(t, x, i)$ and energy current $\vartheta(t, x, i)$. The heat current is the linear combination

$$q(t, x, i) = \vartheta(t, x, i) - \mu_i j(t, x, i) \quad (6)$$

Under this very general assumption about the symmetry content, one can prove[29] that the junction in Figure 1 operates as *energy converter*. To be more explicit, let us consider the operator

$$\dot{Q} = -\sum_{i=1}^{2} q(t, 0, i) \quad (7)$$

and let Φ be any state of the system. Then, if $\langle \dot{Q} \rangle_\Phi < 0$ the junction transforms heat to chemical energy. The opposite process takes place if instead $\langle \dot{Q} \rangle_\Phi > 0$. For a detailed study of this phenomenon of energy transmutation we refer to ref. [29].

An essential role in the general setup is played by the time reversal transformation

$$T j(t, x, i) T^{-1} = -j(-t, x, i) \quad (8)$$

where T is an *anti-unitary* operator. We will show below that in the LB representation

$$\langle j(t, x, i)\rangle_{\mathrm{LB}} \neq -\langle j(-t, x, i)\rangle_{\mathrm{LB}} \quad (9)$$

which implies that the LB state Ω_{LB} is not invariant under time reversal, $T\Omega_{\mathrm{LB}} \neq \Omega_{\mathrm{LB}}$. Consequently, the time reversal symmetry is spontaneously broken in the LB representation. The quantum transport process in the system is therefore irreversible, which gives rise to nontrivial entropy production described by the operator[32–34]

$$\dot{S}(t, x) = -\sum_{i=1}^{2} \beta_i\, q(t, x, i) \quad (10)$$

It is worth mentioning that the currents depend on the lead L_i where they are flowing, thus providing *local* information. The entropy production operator concerns instead the *global* system. Accordingly, the correlation functions (1) refer to a single lead,

**ADVANCED
SCIENCE NEWS**

www.advancedsciencenews.com

annalen
der **physik**

www.ann-phys.org

whereas (2) take into account all the *interference effects* between the heat currents in the two different leads L_1 and L_2.

3. Exactly Solvable System

3.1. The Model

The above considerations have a very general validity. In order to obtain concrete results however, one should fix the dynamics. In choosing among various possibilities, our guiding principle will be to focus on an exactly solvable model, where the zero frequency correlation functions $\mathcal{W}_n[j_i]$ and $\mathcal{W}_n[\dot{S}]$ can be derived in explicit form for all n. For this purpose we consider the bosonic Schrödinger junction with a point-like defect. This system has already been shown[27–29] to be a remarkable laboratory for testing general ideas about quantum transport. The dynamics along the *oriented* leads L_i is fixed by the Schrödinger equation (the natural units $\hbar = c = k_B = 1$ are adopted throughout the paper)

$$\left(i\partial_t + \frac{1}{2m}\partial_x^2\right)\psi(t, x, i) = 0, \qquad x < 0, \quad i = 1, 2 \tag{11}$$

and the canonical commutator

$$[\psi(t, x_1, i_1), \psi^*(t, x_2, i_2)] = \delta_{i_1 i_2}\delta(x_1 - x_2) \tag{12}$$

where $*$ stands for Hermitian conjugation. The defect at $x = 0$, which generates the interaction driving the system out of equilibrium, is fixed by the boundary condition

$$\lim_{x \to 0^-} \sum_{j=1}^{2}\left[\lambda(\mathbb{I} - \mathbb{U})_{ij} + i(\mathbb{I} + \mathbb{U})_{ij}\partial_x\right]\psi(t, x, j) = 0 \tag{13}$$

where $\mathbb{I}$ is the identity matrix, $\mathbb{U}$ is a generic 2×2 unitary matrix, and $\lambda > 0$ is a parameter with dimension of mass. Equation (13) defines the most general contact interaction between the two leads, which ensures[35,36] unitary time evolution (self-adjointness of the bulk Hamiltonian). The associated scattering matrix is[35,36]

$$\mathbb{S}(k) = -\frac{[\lambda(\mathbb{I} - \mathbb{U}) - k(\mathbb{I} + \mathbb{U})]}{[\lambda(\mathbb{I} - \mathbb{U}) + k(\mathbb{I} + \mathbb{U})]} \tag{14}$$

k being the particle momentum. More explicitly

$$\mathbb{S}(k) = \begin{pmatrix} \dfrac{k^2 + ik(\eta_1 - \eta_2)\cos(\vartheta) + \eta_1\eta_2}{(k - i\eta_1)(k - i\eta_2)} & \dfrac{-ie^{i\varphi}k(\eta_1 - \eta_2)\sin(\vartheta)}{(k - i\eta_1)(k - i\eta_2)} \\ \dfrac{-ie^{-i\varphi}k(\eta_1 - \eta_2)\sin(\vartheta)}{(k - i\eta_1)(k - i\eta_2)} & \dfrac{k^2 - ik(\eta_1 - \eta_2)\cos(\vartheta) + \eta_1\eta_2}{(k - i\eta_1)(k - i\eta_2)} \end{pmatrix} \tag{15}$$

where φ and ϑ are arbitrary angles and

$$\eta_i = \lambda\tan(\alpha_i) \tag{16}$$

$(e^{2i\alpha_1}, e^{2i\alpha_2})$ being the eigenvalues of $\mathbb{U}$. The boundary bound states are the poles of (15) located in the upper half plane. We

deduce from (16) that there are at most two bound states. The energy is bounded from below by

$$\omega_{\min} = \min\left\{0, -\theta(\eta_1)\frac{\eta_1^2}{2m}, -\theta(\eta_2)\frac{\eta_2^2}{2m}\right\} \tag{17}$$

where θ is the Heaviside step function.

In the absence of bound states, the general solution of (11)–(13) involves only the scattering component

$$\psi(t, x, i) = \sum_{j=1}^{2}\int_0^\infty \frac{dk}{2\pi}e^{-i\omega(k)t}\Psi_{ij}(k; x)a_j(k) \tag{18}$$

where $\omega(k) = \frac{k^2}{2m}$ is the dispersion relation

$$\Psi(k; x) = \left[e^{-ikx}\mathbb{I} + e^{ikx}\mathbb{S}^*(k)\right], \quad k \geq 0 \tag{19}$$

and the operators $\{a_i(k), a_i^*(k) : k \geq 0, i = 1, 2\}$ generate a standard canonical commutation relation algebra $\mathcal{A}$. If bound states are present, the solution (18) involves an additional term established in ref. [17]. As explained there, this term contributes to the correlation functions (1) and (2), but not to their zero frequency limits (3) and (4), we are focusing on in this paper. For this reason, a potential bound state contribution in (18) can be safely neglected below.

3.2. Basic Observables

Equations (11)–(13) are invariant under $U(1)$-phase transformations and time translations, which imply particle number and total energy conservation. The associated conserved currents are

$$j(t, x, i) = \frac{i}{2m}\left[\psi^*(\partial_x\psi) - (\partial_x\psi^*)\psi\right](t, x, i) \tag{20}$$

and

$$\vartheta(t, x, i) = \frac{1}{4m}[(\partial_t\psi^*)(\partial_x\psi) + (\partial_x\psi^*)(\partial_t\psi) \\ - (\partial_t\partial_x\psi^*)\psi - \psi^*(\partial_t\partial_x\psi)](t, x, i) \tag{21}$$

respectively. In order to derive the correlation functions (1) and (2), one should express $j_x(t, x, i)$ and $\dot{S}(t, x)$ in terms of the generators $\{a_i(k), a_i^*(k)\}$ of the algebra $\mathcal{A}$. Plugging the solution (18) in (20) and (10) one obtains

ADVANCED
SCIENCE NEWS

www.advancedsciencenews.com

annalen
der **physik**

www.ann-phys.org

$$j(t, x, i) = \frac{i}{2m} \int_0^\infty \frac{dk}{2\pi} \int_0^\infty \frac{dp}{2\pi} e^{it[\omega(k) - \omega(p)]}$$

$$\sum_{l,m=1}^2 a_l^*(k) \mathbb{A}_{lm}^i(k, p, x) a_m(p) \tag{22}$$

$$\dot{S}(t, x) = \frac{i}{4m} \int_0^\infty \frac{dk}{2\pi} \int_0^\infty \frac{dp}{2\pi} e^{it[\omega(k) - \omega(p)]}$$

$$\sum_{i,l,m=1}^2 \beta_i [2\mu_i - \omega(k) - \omega(p)] a_l^*(k) \mathbb{A}_{lm}^i(k, p, x) a_m(p) \tag{23}$$

with

$$\mathbb{A}_{lm}^i(k, p, x) \equiv$$

$$\Psi_{li}^*(k; x) [\partial_x \Psi_{im}](p; x) - [\partial_x \Psi_{li}^*](k; x) \Psi_{im}(p; x) \tag{24}$$

The next step toward the derivation of the correlation functions (1), (2) is to fix a representation of the algebra $\mathcal{A}$.

3.3. Correlation Functions in the LB Representation

Studying the physical setup in Figure 1 in a quantum mechanical context, Landauer[7] and Büttiker[8] suggested a nonequilibrium generalization of the Gibbs representation of $\mathcal{A}$ (see e.g., ref. [28]) to systems, which exchange particles and energy with more then one heat reservoir. In what follows we call this generalization the LB representation and refer to ref. [28] for a field theoretical construction of the associated Hilbert space. For deriving the expectation values of (22) and (23) in the LB representation it is enough to compute the $2n$-point function

$$\langle a_{l_1}^*(k_1) a_{m_1}(p_1) \cdots a_{l_n}^*(k_n) a_{m_n}(p_n) \rangle_{\text{LB}} \tag{25}$$

Let us introduce for this purpose the $n \times n$ matrix

$$\mathbb{B}_{ij} = \begin{cases} 2\pi \delta(k_i - p_j) \delta_{l_i m_j} d_{l_i}[\omega(k_i)], & i \leq j \\ 2\pi \delta(k_i - p_j) \delta_{l_i m_j} (1 + d_{l_i}[\omega(k_i)]), & i > j \end{cases} \tag{26}$$

where

$$d_l(\omega) = \frac{1}{e^{\beta_l(\omega - \mu_l)} - 1} \tag{27}$$

is the familiar Bose distribution. Now, using the algebraic construction of the LB representation in ref. [28], one can show that the correlation function (25) is the *permanent* of the matrix $\mathbb{B}$

$$\langle a_{l_1}^*(k_1) a_{m_1}(p_1) \cdots a_{l_n}^*(k_n) a_{m_n}(p_n) \rangle_{\text{LB}} = \text{perm}[\mathbb{B}] \tag{28}$$

It is perhaps useful to recall the explicit form

$$\text{perm}[\mathbb{B}] = \sum_{\sigma_i \in \mathcal{P}_n} \prod_{i=1}^n \mathbb{B}_{i\sigma_i} \tag{29}$$

where $\mathcal{P}_n$ is the set of all permutations of n elements.

By means of (28) and (29) one easily derives the one-point current correlation function

$$\langle j(t, x, i) \rangle_{\text{LB}} = \int_0^\infty \frac{d\omega}{2\pi} \sum_{l=1}^2 \left(\delta_{il} - |\mathbb{S}_{il}(\sqrt{2m\omega})|^2 \right) d_l(\omega) \tag{30}$$

The right hand side of (30) implies (9), establishing a basic characteristic feature of the LB representation—the spontaneous breakdown of time reversal invariance. Let us observe in this respect that the dynamics (11) is time reversal invariant. The same holds for the boundary condition (13), provided that besides being unitary the matrix U is also symmetric.

We would like to comment at this stage on the range of the chemical potentials μ_i. In order to avoid singularities, indicating condensation phenomena, we assume that the particle density $d_l(\omega)$ in the reservoir R_l is positive for all $\omega \geq 0$. Therefore $\mu_l < 0$ in what follows.

3.4. The Zero Frequency Limit

Since at this point the correlation functions (1) and (2) can be treated in the same way, we introduce the notation $\{w_n[\zeta] : \zeta = j_i, \dot{S}; n = 1, 2, \ldots\}$. Time translation invariance implies that $w_n[\zeta]$ depend actually only on the time differences

$$\hat{t}_k \equiv t_k - t_{k+1}, \quad k = 1, \ldots, n-1 \tag{31}$$

which allows to introduce for $n \geq 2$ the frequency ν via the Fourier transform

$$\mathcal{W}_n[\zeta](x_1, \ldots, x_n; \nu) = \int_{-\infty}^\infty d\hat{t}_1 \cdots \int_{-\infty}^\infty d\hat{t}_{n-1}$$

$$e^{-i\nu(\hat{t}_1 + \cdots \hat{t}_{n-1})} w_n[\zeta](t_1, x_1, \ldots, t_n, x_n) \tag{32}$$

Following the classical studies[12–16] of the fermionic quantum noise, which have been extended in ref. [24] to the current cumulants with $n > 2$ and applied in the framework of full counting statistics,[18–27] we perform the zero frequency limit

$$\mathcal{W}_n[\zeta] = \lim_{\nu \to 0^+} \mathcal{W}_n[\zeta](x_1, \ldots, x_n; \nu) \tag{33}$$

In the limit (33) the quantum fluctuations are integrated over the whole time axes and it turns out that the position dependence drops out. Because of this relevant simplification, the zero frequency regime is intensively explored also in experiments.

The derivation of $\mathcal{W}_n[j_i]$ and $\mathcal{W}_n[\dot{S}]$ in explicit form is straightforward but long. For this reason we summarize below only the main steps of the procedure:

(i) using (22), and (24) and (28) one first obtains a representation of the correlation function $w_n[\zeta](t_1, x_1, \ldots, t_n, x_n)$, involving n integrations over k_i and n integrations over p_j;

(ii) by means of the delta functions in (26) one eliminates all n integrals in p_j;

(iii) plugging the obtained expression in (32), one performs all $(n - 1)$ integrals in $\hat{t}_i$;

(iv) at $\nu = 0$ the latter produce $(n-1)$ delta functions, which allow to eliminate all the integrals over k_i except one, for instance that over $k_1 = k$;

(v) since now the matrix (24) must be evaluated at $k = p$, the x dependence drops out and one finds

$$\mathbb{A}^i_{lm}(k, k, x) = -2k[\delta_{li}\delta_{ij} - \mathbb{S}_{li}(k)\overline{\mathbb{S}}_{ji}(k)] \qquad (34)$$

the bar indicating complex conjugation;

(vi) switch to the variable $\omega = k^2/2m$ in the integral over k;

(vii) introduce the 2×2 matrix

$$\mathbb{J}_{11}(\omega) = -\mathbb{J}_{22}(\omega) = |\mathbb{S}_{12}(\sqrt{2m\omega})|^2 \equiv \tau(\omega) \qquad (35)$$

$$\mathbb{J}_{12}(\omega) = \overline{\mathbb{J}}_{21}(\omega) = -\mathbb{S}_{11}(\sqrt{2m\omega})\overline{\mathbb{S}}_{12}(\sqrt{2m\omega}) \qquad (36)$$

where $\tau(\omega)$ is the *transmission probability*;

(viii) introduce finally the $n \times n$ matrix

$$\mathbb{D}_{ij}(\omega; l_1, \dots, l_n)$$
$$= \begin{cases} \mathbb{J}_{l_j l_i}(\omega) d_{l_j}(\omega), & i \le j \\ \mathbb{J}_{l_j l_i}(\omega) d_{l_j}(\omega)\left[1 + d_{l_i}(\omega)\right], & i > j \end{cases} \qquad (37)$$

and define the sum of permanents

$$\mathcal{K}_n(\omega) = \sum_{l_1, \dots, l_n = 1}^{2} \operatorname{perm}[\mathbb{D}(\omega; l_1, \dots, l_n)] \qquad (38)$$

Using the matrix (37) and the definition (29) of permanent, one can explicitly derive each term of the sequence $\{\mathcal{K}_n(\omega) : n = 1, 2, \dots\}$, which will play an important role in what follows. The first few terms are

$$\mathcal{K}_1(\omega) = \tau(\omega)c_1(\omega)$$
$$\mathcal{K}_2(\omega) = \tau(\omega)\left[c_2(\omega) + 2c_1^2(\omega)\tau(\omega)\right]$$
$$\mathcal{K}_3(\omega) = \tau^2(\omega)c_1(\omega)\left[1 + 6c_2(\omega) + 6c_1^2(\omega)\tau(\omega)\right] \qquad (39)$$

where c_i are the frequently used below combinations

$$c_1(\omega) = d_1(\omega) - d_2(\omega) \qquad (40)$$

$$c_2(\omega) = d_1(\omega) + d_2(\omega) + 2d_1(\omega)d_2(\omega) \qquad (41)$$

Performing the above eight steps, one obtains for the particle current the integral representation (3) with

$$\mathcal{M}_n[j_1] = \mathcal{K}_n(\omega) \qquad (42)$$

$$\mathcal{M}_n[j_2] = (-1)^n \mathcal{K}_n(\omega) \qquad (43)$$

and for the entropy production (4) with

$$\mathcal{M}_n[\dot{S}] = [\gamma_{21}(\omega)]^n \mathcal{K}_n(\omega) \qquad (44)$$

where

$$\gamma_{ij}(\omega) = (\beta_i - \beta_j)\omega - (\beta_i \mu_i - \beta_j \mu_j) \qquad (45)$$

As already observed in the introduction, $\mathcal{M}_n[j_i]$ and $\mathcal{M}_n[\dot{S}]$ given by (42)–(44), are the moments of the probability distributions $\varrho[j_i]$ and $\varrho[\dot{S}]$. The goal of the next section is to reconstruct these distributions from the moments and uncover the physical information codified therein.

4. Probability Distributions

4.1. Moment Generating Functions

The general problem now is to find a function $\varrho[\zeta]$ such that

$$\mathcal{M}_n[\zeta] = \int_{-\infty}^{\infty} d\sigma \, \sigma^n \varrho[\zeta](\sigma), \qquad n = 0, 1, \dots \qquad (46)$$

where $\mathcal{M}_n[\zeta]$ are given for $n \ge 1$ by (42)–(44) and

$$\mathcal{M}_0[\zeta] = 1 \qquad (47)$$

is a normalization condition. As is well known,[37] $\varrho[\zeta]$ is given by the Fourier transform

$$\varrho[\zeta](\sigma) = \int_{-\infty}^{\infty} \frac{d\lambda}{2\pi} \, e^{-i\lambda\sigma} \, \chi[\zeta](\lambda) \qquad (48)$$

of the moment generating function

$$\chi[\zeta](\lambda) = \sum_{n=0}^{\infty} \frac{(i\lambda)^n}{n!} \mathcal{M}_n[\zeta] \qquad (49)$$

We will proceed therefore by determining first $\chi[\zeta]$ from the corresponding moments, given by (42)–(44), and after that performing the Fourier transform (48).

For deriving the moment generating function $\chi[j_1](\lambda)$ in explicit form we apply to our case the technique, developed by Glauber in quantum optics for the counting statistics of photons (see e.g., ref. [38]). First we introduce two auxiliary bosonic oscillators $\{a_i^*, a_i, : i = 1, 2\}$, satisfying the commutation relations

$$[a_i, a_j^*] = \delta_{ij}, \qquad [a_i^*, a_j^*] = [a_i, a_j] = 0 \qquad (50)$$

Using these oscillators one can generate the sum of permanents in the right hand side of (38). In fact, setting

$$K(\omega) = \sum_{i=1}^{2} a_i^* \mathbb{K}_{ij}(\omega) a_i, \qquad J(\omega) = \sum_{i,j=1}^{2} a_i^* \mathbb{J}_{ij}(\omega) a_j \qquad (51)$$

where

$$\mathbb{K}_{ij}(\omega) = \beta_i(\omega - \mu_i)\delta_{ij} \qquad (52)$$

and $\mathbb{J}(\omega)$ is given by (35) and (36), one can verify by means of (50) that

$$\sum_{l_1, \dots, l_n = 1}^{2} \operatorname{perm}[\mathbb{D}(\omega; l_1, \dots, l_n)] = \frac{\operatorname{Tr}\left[e^{-K(\omega)} J(\omega)^n\right]}{\operatorname{Tr}\left[e^{-K(\omega)}\right]} \qquad (53)$$

ADVANCED
SCIENCE NEWS

www.advancedsciencenews.com

annalen
der physik

www.ann-phys.org

Equations (38), (42), (49), and (53) now imply the following trace representation for the moment generating function

$$\chi[j_1](\lambda) = \frac{\text{Tr}\left[e^{-K(\omega)}e^{i\lambda J(\omega)}\right]}{\text{Tr}\left[e^{-K(\omega)}\right]} \tag{54}$$

Observing that

$$[K(\omega), J(\omega)] = \sum_{i,j=1}^{2} a_i^* \left([\mathbb{K}, \mathbb{J}]\right)_{ij} a_j \tag{55}$$

one can apply the result of ref. [23] for traces of the type (54) and obtain the alternative determinant representation

$$\chi[j_1](\lambda) = \frac{\det\left[1 - e^{\mathbb{K}(\omega)}\right]}{\det\left[1 - e^{\mathbb{K}(\omega)}e^{i\lambda\mathbb{J}(\omega)}\right]}$$

$$= \frac{1}{\det\left[1 - (1 - e^{\mathbb{K}(\omega)})^{-1}e^{\mathbb{K}(\omega)}(e^{i\lambda\mathbb{J}(\omega)} - 1)\right]} \tag{56}$$

which is more manageable. Indeed, using that

$$\left[\left(1 - e^{\mathbb{K}(\omega)}\right)^{-1}e^{\mathbb{K}(\omega)}\right]_{ij} = d_i(\omega)\delta_{ij} \tag{57}$$

and once again the explicit form (35) and (36) of the matrix $\mathbb{J}(\omega)$, one finally gets

$$\chi[j_1](\lambda) = \frac{1}{1 - ic_1\sqrt{\tau}\sin(\lambda\sqrt{\tau}) - c_2[\cos(\lambda\sqrt{\tau}) - 1]} \tag{58}$$

For conciseness we omit here and in what follows the dependence of τ and c_i on the energy ω.

Analogously, for the entropy production generating function one finds

$$\chi[\dot{S}](\lambda) = \frac{1}{1 - ic_1\sqrt{\tau}\sin(\lambda\gamma_{21}\sqrt{\tau}) - c_2[\cos(\lambda\gamma_{21}\sqrt{\tau}) - 1]} \tag{59}$$

According to (48) the probability distributions $\varrho[j_1]$ and $\varrho[\dot{S}]$, we are looking for, are obtained by performing the Fourier transform of (58) and (59).

4.2. Particle Current Distribution

Since the right hand side of (58) is a periodic function with period $2\pi/\sqrt{\tau}$, the generating function has the Fourier expansion

$$\chi[j_1](\lambda) = \sum_{k=-\infty}^{\infty} p_k\, e^{ik\lambda\sqrt{\tau}} \tag{60}$$

The coefficients $\{p_{\pm n} : n = 0, 1, \ldots\}$ can be deduced from (58) and read

$$p_{\pm n} = \frac{c_\pm^n}{1 + c_2} \sum_{j=0}^{\infty} \binom{2j + n}{j}(c_+ c_-)^j \tag{61}$$

where

$$c_\pm = \frac{(c_2 \pm c_1\sqrt{\tau})}{2(1 + c_2)} \tag{62}$$

Using $\mu_i < 0$ and $0 \le \tau \le 1$ one can show that

$$c_2 > 0, \qquad c_\pm > 0, \qquad c_\pm < 1, \qquad c_+ c_- < 1/4 \tag{63}$$

which imply that the series (61) is convergent and $p_k > 0$ for all k. Indeed, in closed form one has the Gauss hypergeometric function

$$p_{\pm n} = \frac{c_\pm^n}{1 + c_2}\, {}_2F_1\left[\frac{1 + n}{2}, \frac{2 + n}{2}, n + 1, 4c_+ c_-\right] > 0 \tag{64}$$

From (60) one deduces that the probability distribution $\varrho[j_1]$ is the *Dirac comb* function

$$\varrho[j_1](\xi) = \sum_{k=-\infty}^{\infty} p_k\, \delta(\xi - k\sqrt{\tau}) \tag{65}$$

where the weights p_k are given by (64) and satisfy

$$\sum_{k=-\infty}^{\infty} p_k = 1 \tag{66}$$

In fact, (58) implies on the one hand

$$\int_{-\infty}^{\infty} d\xi\, \varrho[j_1](\xi) = \chi[j_1](0) = 1 \tag{67}$$

On the other hand, integrating (65) one gets

$$\int_{-\infty}^{\infty} d\xi\, \varrho[j_1](\xi) = \sum_{k=-\infty}^{\infty} p_k \tag{68}$$

which completes the argument. Summarizing, since in addition $p_k > 0$, the coefficients p_k represent probabilities, whose physical meaning will be uncovered below.

Finally, using (43) one concludes that

$$\chi[j_2](\lambda) = \chi[j_1](-\lambda) \tag{69}$$

which implies in turn that

$$\varrho[j_2](\xi) = \varrho[j_1](-\xi) \tag{70}$$

Equivalently, $\varrho[j_1]$ and $\varrho[j_2]$ are related by

$$p_k \mapsto p_{-k} \tag{71}$$

4.3. Entropy Production Distribution

Employing (59), a straightforward extension of the analysis in the previous subsection leads to

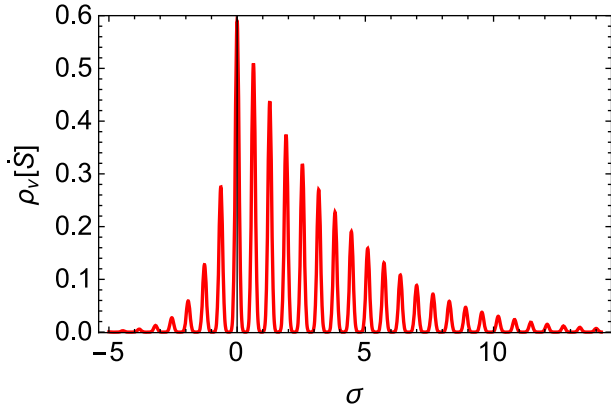$$\varrho[\dot{S}](\sigma) = \sum_{k=-\infty}^{\infty} p_k\, \delta(\sigma - k\gamma_{21}\sqrt{\tau}) \tag{72}$$

**ADVANCED
SCIENCE NEWS**

www.advancedsciencenews.com

*annalen
der* **physik**

www.ann-phys.org

Figure 2. The smeared distribution ϱ_ν with $\nu = 200$, $\gamma_1 = 1$, $\gamma_2 = 0.1$ and $\tau = 1/2$.

with the same probabilities $p_{\pm n}$ given by (64). This property is the first indication that the probabilities $\{p_{\pm n} : n = 0, 1 \ldots\}$ carry universal and fundamental information about the quantum transport at the microscopic level. We postpone the detailed discussion of this issue to the next subsection, focussing here on the possibility to illustrate graphically the behavior of the distribution (72). For this purpose it is convenient to introduce the δ-sequence

$$\delta_\nu(\sigma) = \frac{\nu}{\sqrt{\pi}} e^{-\nu^2 \sigma^2}, \qquad \nu > 0 \tag{73}$$

and the smeared distribution

$$\varrho_\nu[\dot{S}](\sigma) = \sum_{k=-\infty}^{\infty} p_k \, \delta_\nu(\sigma - k \, \gamma_{21} \sqrt{\tau}) \tag{74}$$

As is well known, for $\nu \to \infty$ one has $\varrho_\nu \to \varrho$ in the sense of generalized functions. The plot of ϱ_ν, reported in **Figure 2**, nicely illustrates the physics discussed in the next subsection.

4.4. Physical Interpretation of the Probabilities p_k

It is instructive in this section to restore the electric charge e in the current (20) by $j \mapsto ej$. The distribution (65) now takes the form

$$\varrho[j_1](\xi) = \sum_{k=-\infty}^{\infty} p_k \, \delta(\xi - ke\sqrt{\tau}) \tag{75}$$

where the parameter ξ measures the charge which is transferred between the two reservoirs. Without loss of generality we can assume that ξ is positive if the particles are emitted from R_2 and absorbed by R_1 and is negative for the process in the opposite direction. The argument of the delta function in (75) suggest a simple interplay between the transport on the one hand and the processes of emission and absorption on the other hand. Suppose that R_2 emits in the system the charge ke. Because of the defect, the part $ke\sqrt{\tau}$ is transmitted and absorbed by R_1. The rest $ke(1 - \sqrt{\tau})$ is reflected by the defect and reabsorbed by R_2.

This is a purely quantum scattering effect. For $\tau = 1$ the defect is fully transparent and the charge emitted from one reservoir is totally absorbed by the other one. Finally, the term $k = 0$ in (75) describes the emission and absorption of particles by the same reservoir, thus corresponding to a vanishing charge transfer $\xi = 0$.

Summarizing, the probabilities p_k fully characterize the elementary processes of particle emission and absorption by the heat reservoirs, which provide in turn the common basis for all types of transport in the junction. In fact, the probability distributions for the energy and heat currents ϑ_1 and q_1 in the lead L_1 are obtained from (75) by the substitution

$$e \longmapsto \begin{cases} \omega, & \text{for} \quad \varrho[\vartheta_1] \\ \omega - e\mu_1, & \text{for} \quad \varrho[q_1] \end{cases} \tag{76}$$

which confirms the universal character of the the probabilities p_k.

4.5. Microscopic Quantum Version of the Second Law

From (74) one infers for the entropy production the values $\{\sigma_k = k\gamma_{21}\sqrt{\tau} : k = 0, \pm 1, \pm 2, \ldots\}$. Suppose now that $\gamma_{21} > 0$. Accordingly, we call R_2 the "hot" reservoir and R_1 the "cold" one. In this case we deduce from (72) that p_k with $k > 0$ are associated with the transmission from the hot reservoir to the cold one, leading to positive entropy production $\sigma_k = k\gamma_{21}\sqrt{\tau} > 0$. For $k < 0$ instead, p_k correspond to the transport from the cold to the hot reservoir, which generates negative entropy production $\sigma_k = k\gamma_{21}\sqrt{\tau} < 0$. For $k = 0$ there is no particle exchange between the two reservoirs and consistently the entropy production vanishes.

Analyzing $c_\pm$, given by (62), it is easy to show that for $k > 0$

$$\gamma_{21} > 0 \implies c_+ > c_- \implies p_k > p_{-k} \tag{77}$$

The processes with positive entropy production thus dominate that with the negative one. This feature is illustrated in Figure 2 and suggests that as in the fermionic case[30] all moments (44) of the probability distribution (72) are non-negative (5). For proving this bound we denote by $\Delta(\lambda)$ the denominator of $\chi[\dot{S}](\lambda)$, given by (59), and observe that

$$\Delta(-i\lambda) = 1 - c_1\sqrt{\tau}\sinh(\lambda\gamma_{21}\sqrt{\tau}) - c_2[\cosh(\lambda\gamma_{21}\sqrt{\tau}) - 1]$$

$$= \sum_{n=0}^{\infty} \lambda^n a_n \tag{78}$$

where

$$a_n = \begin{cases} 1, & n = 0 \\ -\dfrac{\gamma_{21}^{2k-1}\tau^k}{(2k-1)!} c_1, & n = 2k - 1 \\ -\dfrac{\gamma_{21}^{2k}\tau^k}{(2k)!} c_2, & n = 2k \end{cases} \tag{79}$$

On the other hand

$$\chi[\dot{S}](-i\lambda) = \sum_{n=0}^{\infty} \lambda^n b_n, \qquad b_n = \frac{\mathcal{M}_n[\dot{S}]}{n!} \tag{80}$$

and using the identity

$$\Delta(-i\lambda)\chi[\dot{S}](-i\lambda) = 1 \tag{81}$$

one gets for $n \geq 1$ the recursive relation

$$b_n = -a_n - a_{n-1}b_1 - a_{n-2}b_2 - \cdots - a_1 b_{n-1} \tag{82}$$

with

$$b_0 = \mathcal{M}_0[\dot{S}] = 1 \tag{83}$$

At this point the inequality $\mathcal{M}_n[\dot{S}] \geq 0$ follows from (82) by induction, observing that $\mu_i < 0$ implies that

$$\gamma_{21}c_1 \geq 0, \quad c_2 \geq 0 \implies a_n \leq 0, \qquad \forall\, n \geq 1 \tag{84}$$

For the even moments $\mathcal{M}_{2k}[\dot{S}]$ this feature is a direct consequence of the fact that (72) is a probability distribution ($0 < p_k < 1$), but for the odd ones $\mathcal{M}_{2k-1}[\dot{S}]$, this is not at all automatic and represents a characteristic feature of the distribution $\varrho[\dot{S}]$, governing the entropy production fluctuations. Since $\mathcal{M}_1[\dot{S}]$ is the mean value of the entropy production, the bound (5) can be interpreted[30] as a quantum counterpart of the second law of thermodynamics for a system in a fixed steady state, which implements the contact with two heat reservoirs as shown in Figure 1. We would like to mention in this respect that a quantum version of the second law, relative to the transition between different states of a system in contact with one heat bath, has been proposed in refs. [39,40]. In that case there is actually a whole family of "second laws," each of them enforcing a specific physical constraint on the thermodynamic evolution.

We conclude this section by an observation concerning the influence of a hypothetical *classical* measuring devise on the system under consideration. The simplest way to implement such a devise is to introduce[21–25] in (11) a minimal coupling $i\partial_x \longmapsto i\partial_x + A(x)$ with a suitable *classical* external field $A(x)$. The study of this new setup can be performed following mutatis mutandis the above analysis and is beyond the scope of this paper, focussed exclusively on the quantum behavior. In the fermionic case the impact of a classical field $A(x) \sim \delta(x)$ on $\varrho[j_i]$ and $\varrho[\dot{S}]$ has been discussed in detail in refs. [22] and [27], respectively.

5. Efficiency

At the quantum level the question of efficiency has been addressed in the past mainly by studying the mean value $\langle q(t, x, i)\rangle_{\text{LB}}$ of the heat currents in the two leas L_i. Unfortunately, $\langle q(t, x, i)\rangle_{\text{LB}}$ does not keep trace of the quantum fluctuations, which are expected to affect the quantum efficiency and whose presence is actually the relevant novelty with respect to the classical case.

Our main objective here is to introduce and study a suitable quantity, which describes the transport efficiency at the microscopic level and captures the quantum fluctuations. To this end we use the set of probabilities $\{p_k : k = 0, \pm 1, \pm 2, \ldots\}$ derived above and take advantage of the fact that our formalism provides the values of the positive and negative entropy productions $\sigma_{\pm}^{\text{tot}}$ separately and not only the value of their sum $\sigma_{+}^{\text{tot}} + \sigma_{-}^{\text{tot}}$. In fact, the probability distribution (72) implies that for $\gamma_{21} > 0$ the probabilities $p_{n \geq 1}$ and $p_{n \leq -1}$ correspond to positive and negative entropy productions, respectively. For $\gamma_{21} < 0$ one has that $p_{n \geq 1}$ and $p_{n \leq -1}$ exchange their role. Therefore

$$\sigma_{\pm}(\omega) = \pm\theta(\gamma_{12})\gamma_{12}\sqrt{\tau}\sum_{n=1}^{\infty} n\, p_{\mp n} \pm \theta(\gamma_{21})\gamma_{21}\sqrt{\tau}\sum_{n=1}^{\infty} n\, p_{\pm n} \tag{85}$$

give the positive and negative entropy productions at energy ω. Consequently, the total positive/negative entropy production in the system is

$$\sigma_{\pm}^{\text{tot}} = \int_0^{\infty} d\omega\, \sigma_{\pm}(\omega) \tag{86}$$

Because of (77) one has

$$\sigma_{+}(\omega) > -\sigma_{-}(\omega) > 0 \implies \sigma_{+}^{\text{tot}} > -\sigma_{-}^{\text{tot}} > 0 \tag{87}$$

The main idea now is to extend and adapt the concept of *second law* macroscopic efficiency (see e.g., ref. [31]) for heat engines to our case. In order to recall briefly this concept, let us consider for a moment a classical heat engine in contact with two heat baths as shown in Figure 1. Let us denote the work transfer rate of the engine by $\dot{W} > 0$. Moreover, let $\dot{W}_{\text{rev}}$ be the value of $\dot{W}$ in the limit of reversible operation. Then, the second law efficiency is defined by[31]

$$\eta_{\text{II}} = \frac{\dot{W}}{\dot{W}_{\text{rev}}} \tag{88}$$

It is perhaps useful to recall also that the more familiar *first law* efficiency η_{I} is given in terms of η_{II} by[31]

$$\eta_{\text{I}} = \eta_{\text{II}}(1 - r), \qquad r \equiv \frac{\beta_1}{\beta_2}, \qquad \beta_2 \geq \beta_1 \tag{89}$$

The second law of thermodynamics states that $\dot{W} \leq \dot{W}_{\text{rev}}$, implying $\eta_{\text{II}} \leq 1$. The value $\eta_{\text{II}} = 1$ is reached in the limit of reversibility. This is the fundamental property we would like to preserve when introducing a concept of efficiency for the quantum transport in the junction in Figure 1, where instead of the work transfer rates $\dot{W}$ and $\dot{W}_{\text{rev}}$, we know the entropy productions $\sigma_{\pm}^{\text{tot}}$. At this point the quantum second law in the form (87) suggests to consider the quantity

$$\varepsilon_{\text{II}} = -\frac{\sigma_{-}^{\text{tot}}}{\sigma_{+}^{\text{tot}}} \tag{90}$$

which satisfies $0 \leq \varepsilon_{\text{II}} \leq 1$ and has the desired reversibility limit

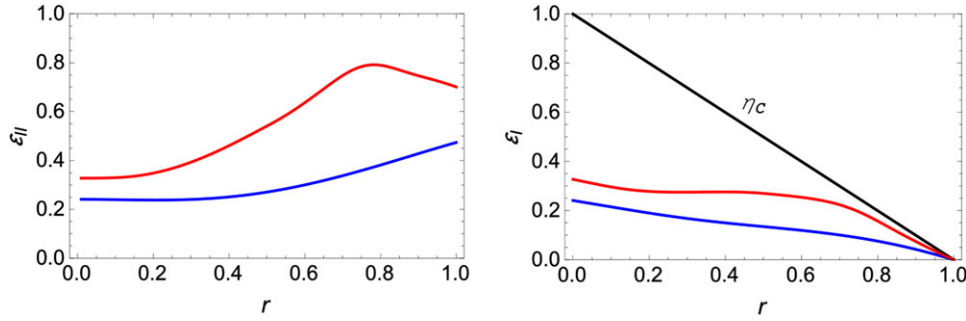$$\sigma_{+}^{\text{tot}} + \sigma_{-}^{\text{tot}} = 0 \implies \varepsilon_{\text{II}} = 1 \tag{91}$$

**ADVANCED
SCIENCE NEWS**
www.advancedsciencenews.com

annalen
der **physik**
www.ann-phys.org

Figure 3. The efficiencies ε_{II} (left panel) and ε_I (right panel) for $\mu_1 = -0.1$ and $\mu_2 = -0.5$ (blue line) and $\mu_1 = -0.4$ and $\mu_2 = -0.2$ (red line) at $\beta_1 = 2$ and $\tau = 0.2$. The black line is the Carnot efficiency.

In addition, setting

$$\varepsilon_I = \varepsilon_{II}(1-r) = -\frac{\sigma_-^{tot}}{\sigma_+^{tot}}(1-r) \qquad (92)$$

we conclude that, as in the case of heat engines, ε_I can not exceed the familiar Carnot efficiency $\eta_C = 1 - r$, recovered in the regime (91) of reversibility.

The analytic study of (90) and (92) for generic values of the heat bath parameters is rather complicated. Fortunately however, numerics works quite well. This fact is illustrated in **Figure 3**, where ε_{II} and ε_I are plotted for different values of μ_i. The blue and red lines display the typical behaviour for $\mu_2 < \mu_1 < 0$ and $\mu_1 < \mu_2 < 0$, respectively.

Finally, we would like to stress that the efficiency ε_{II} applies to both regimes of operation of the quantum junction as a converter of heat to chemical energy or vice versa.

6. Role of Statistics—Comparison with Fermions

In the fermionic case, the Pauli exclusion principle simplifies the picture. In fact, the $n \geq 2$ emission/absorption processes with the same energy are forbidden and the fermionic distribution $\varrho^f[j_1]$ involves three terms only.

$$\varrho^f[j_1](\xi) = \sum_{k=-1}^{1} p_k^f \, \delta(\xi - k\sqrt{\tau}) \qquad (93)$$

The three "teeth" of the Dirac comb (93) are

$$p_{\pm 1}^f = \frac{1}{2}\left(c_2^f \mp c_1^f\sqrt{\tau}\right), \qquad p_0^f = 1 - c_2^f \qquad (94)$$

where

$$c_1^f \equiv d_1^f - d_2^f, \qquad c_2^f \equiv d_1^f + d_2^f - 2d_1^f d_2^f \qquad (95)$$

and

$$d_i^f(\omega) = \frac{1}{e^{\beta_i(\omega-\mu_i)}+1} \qquad (96)$$

is the Fermi distribution. It is easily seen that

$$p_{-1}^f + p_0^f + p_1^f = 1, \qquad p_{\pm 1}^f \in [0,1], \qquad p^f \in [0,1] \qquad (97)$$

which imply that $\varrho^f[j_1]$ is a true probability distribution.

In terms of the probabilities (94) the fermionic entropy production distribution takes the form[30]

$$\varrho^f[\dot{S}](\sigma) = \sum_{k=-1}^{1} p_k^f \, \delta(\sigma - k\,\gamma_{21}\sqrt{\tau}) \qquad (98)$$

The relative moments ($k = 1, 2, ...$)

$$\mathcal{M}_{2k-1}^f[\dot{S}] = \tau^k \gamma_{21}^{2k-1} c_1^f \qquad (99)$$

$$\mathcal{M}_{2k}^f[\dot{S}] = \tau^k \gamma_{21}^{2k} c_2^f \qquad (100)$$

are much simpler than the bosonic ones (38) and (44) and satisfy the bound $\mathcal{M}_n^f[\dot{S}] \geq 0$ implementing the second law.

The difference between the nonequilibrium transport of bosons and fermions emerges also by comparing the relative efficiencies. From (98) one infers the entropy productions

$$\sigma_\pm^f(\omega) = \pm\theta(\gamma_{12})\gamma_{12}\sqrt{\tau}\,p_{\mp 1}^f \pm \theta(\gamma_{21})\gamma_{21}\sqrt{\tau}\,p_{\pm 1}^f \qquad (101)$$

Substituting (101) in (86) one obtains the fermionic versions ε_I^f and ε_{II}^f of the first and second law efficiencies, which differ from the bosonic ones. **Figure 4** displays a comparison between ε_{II}^f and its bosonic counterpart ε_{II} at the same heat bath parameters. In the left panel ε_{II}^f exceeds ε_{II}. For the same chemical potentials, but at higher temperature $1/\beta_1$ in the right panel there is an interval in r for which $\varepsilon_{II} > \varepsilon_{II}^f$.

7. Discussion

The main goal of the present paper is to develop a microscopic approach to nonequilibrium transport, which takes into account in a systematic way the quantum fluctuations at any order. The basic idea is to use the probability distributions $\varrho[j_i]$ and $\varrho[\dot{S}]$, generated respectively by the n-point correlation functions of the particle current and entropy production operators for all $n \geq 1$. We have shown that these distributions determine a sequence
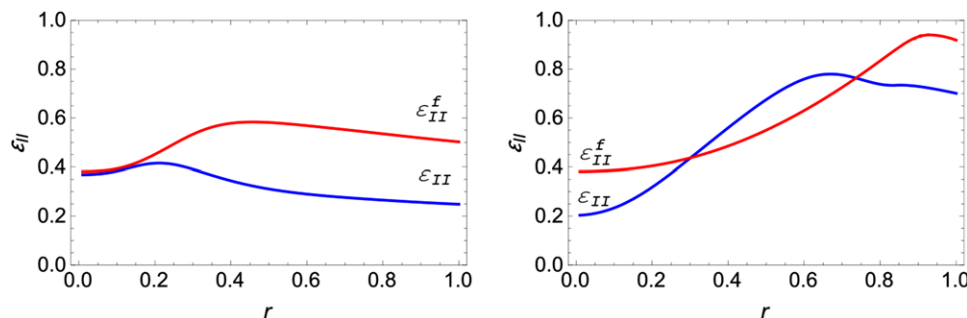
**ADVANCED
SCIENCE NEWS**
www.advancedsciencenews.com

annalen
der **physik**
www.ann-phys.org

Figure 4. The fermionic efficiency $\varepsilon_{\mathrm{II}}^{\mathrm{f}}$ (red line) and the bosonic efficiency $\varepsilon_{\mathrm{II}}$ (blue line) for $\mu_1 = -20$, $\mu_2 = -1$, and $\tau = 0.2$ at $\beta_1 = 0.1$ (left panel) and $\beta_1 = 0.01$ (right panel).

of probabilities $\{p_k(\omega) : k = 0, \pm 1, \pm 2, \ldots\}$ associated with the fundamental microscopic processes of emission and absorption of particles from the heat reservoirs, driving the system away from equilibrium. It turns out that these probabilities fully describe the particle, energy, and heat transport. Moreover, they determine the quantum entropy production and characterize the efficiency at the microscopic level, thus providing universal information about the system.

The above general ideas, which have been illustrated in the paper on the example of an exactly solvable model, suggest different promising directions for further research. First of all, it will be interesting to lift the zero frequency condition and evaluate the distributions $\varrho[j_i]$ and $\varrho[\dot{S}]$ in general. In this respect, the study[27] of the second moment $\mathcal{M}[j_i]$ at arbitrary finite frequency indicated for instance the relevant impact of bound states on the particle transport. This result implies that the recent experimental progress[41–43] in finite frequency quantum transport can provide a new valuable tool for bound state spectroscopy.

A further challenging question in the above context concerns the interactions. Since our exactly solvable system involves only a boundary interaction at the junction, one may wonder about the role of bulk interactions. In this respect the analysis of ref. [44] represents a starting point for the study of the nonequilibrium Luttinger liquid. Another recently investigated[45] example is the Lieb–Liniger model with contact repulsive interactions. The results of ref. [45] concern the probability distribution $\varrho[\psi^*\psi]$, generated by the particle density operator $\psi^*\psi$, and are obtained in a specific nonequilibrium regime. It is worth mentioning that also in that case $\varrho[\psi^*\psi]$ is a Dirac comb distribution, whose coefficients are the counterparts of our probabilities (64). It will be interesting to study the entropy production in the Lieb–Liniger case, exploring the influence of the bulk interactions on the positivity of the mean entropy production and the higher moments of the associated distribution.

Acknowledgements

Conflict of Interest

The authors declare no conflict of interest.

[1] I. Bloch, J. Dalibard, W. Zwerger, *Rev. Mod. Phys.* **2008**, *80*, 885.
[2] M. A. Cazalilla, R. Citro, T. Giamarchi, E. Orignac, M. Rigol, *Rev. Mod. Phys.* **2011**, *83*, 1405.
[3] F. Chevy, C. Salomon, *J. Phys. B: At. Mol. Opt. Phys.* **2016**, *49*, 192001.
[4] A. Micheli, A. J. Daley, D. Jaksch, P. Zoller, *Phys. Rev. Lett.* **2004**, *93*, 140408.
[5] J. A. Stickney, D. Z. Anderson, A. A. Zozulya, *Phys. Rev. A* **2007**, *75*, 013608.
[6] R. A. Pepino, J. Cooper, D. Meiser, D. Z. Anderson, M. J. Holland, *Phys. Rev. A* **2010**, *82*, 013640.
[7] a) R. Landauer, *IBM J. Res. Dev.* **1957**, *1*, 233; b) R. Landauer, *Philos. Mag.* **1970**, *21*, 863.
[8] a) M. Büttiker, *Phys. Rev. Lett.* **1986**, *57*, 1761; b) M. Büttiker, *IBM J. Res. Dev.* **1988**, *32*, 317.
[9] P. W. Anderson, D. J. Thouless, A. Abrahams, D. S. Fisher, *Phys. Rev. B* **1980**, *22*, 3519.
[10] D. S. Fisher, P. A. Lee, *Phys. Rev. B* **1981**, *23*, 6851.
[11] U. Sivan, Y. Imry, *Phys. Rev. B* **1986**, *33*, 551.
[12] Th. Martin, R. Landauer, *Phys. Rev. B* **1992**, *45*, 1742.
[13] M. Büttiker, *Phys. Rev. B* **1992**, *46*, 12485.
[14] M. J. M. de Jong, C. W. J. Beenakker, in *Mesoscopic Electron Transport* (Eds: L. L. Sohn, L. P. Kouwenhoven, G. Schoen), NATO ASI Series 345 Kluwer Academic Publishers, Dordrecht, The Netherlands **1997**, p. 225.
[15] Ya. M. Blanter, M. Büttiker, *Phys. Rep.* **2000**, *336*, 1.
[16] M. Mintchev, L. Santoni, P. Sorba, *J. Phys. A* **2015**, *48*, 285002.
[17] M. Mintchev, L. Santoni, P. Sorba, *Ann. Phys. (Berlin)* **2017**, *529*, 1600274.
[18] V. K. Khlus, *Sov. Phys. JETP* **1987**, *66*, 1243.
[19] G. B. Lesovik, *JETP Lett.* **1989**, *49*, 592.
[20] L. S. Levitov, G. B. Lesovik, *JETP Lett.* **1992**, *55*, 555.
[21] L. S. Levitov, H. Lee, G. B. Lesovik, *J. Math. Phys.* **1996**, *37*, 4845.
[22] G. B. Lesovik, N. M. Chtchelkatchev, *JETP Lett.* **2003**, *77*, 393.
[23] I. Klich, in *Quantum Noise in Mesoscopic Physics* (Ed: Y. V. Nazarov), Kluwer Academic Publishers, Dordrecht, The Netherlands **2003**, p. 397.
[24] D. B. Gutman, Y. Gefen, A. D. Mirlin, in *Quantum Noise in Mesoscopic Physics* (Ed: Y. V. Nazarov), Kluwer Academic Publishers, Dordrecht, The Netherlands **2003**, p. 497.

[25] M. Esposito, U. Harbola, S. Mukamel, *Rev. Mod. Phys.* **2009**, *81*, 1665.

[26] P. Gaspard, *Ann. Phys. (Berlin)* **2015**, *527*, 663.

[27] M. Mintchev, L. Santoni, P. Sorba, *J. Phys. A* **2016**, *49*, 265002.

[28] M. Mintchev, *J. Phys. A* **2011**, *44*, 415201.

[29] M. Mintchev, L. Santoni, P. Sorba, *J. Phys. A* **2015**, *48*, 055003.

[30] M. Mintchev, L. Santoni, P. Sorba, *Phys. Rev. E* **2017**, *96*, 052124.

[31] A. Bejan, *Advanced Engineering Thermodynamics*, John Wiley and Sons, Hoboken, NJ, USA **2016**.

[32] H. B. Callen, *Thermodynamics and an Introduction to Thermostatistics*, John Wiley and Sons, New York **1960**.

[33] V. Jaksič, C.-A. Pillet, *Comm. Math. Phys.* **2001**, *217*, 285.

[34] G. Nenciu, *J. Math. Phys.* **2007**, *48*, 033302.

[35] V. Kostrykin, R. Schrader, *Fortschr. Phys.* **2000**, *48*, 703.

[36] M. Harmer, *J. Phys. A* **2000**, *33*, 9015.

[37] J. A. Shohat, J. D. Tamarkin, *The Problem of Moments*, American Mathematical Society, Providence, RI, USA **1970**.

[38] R. J. Glauber, *Quantum Theory of Optical Coherence*, Wiley-VCH, Weinheim, Germany **2007**.

[39] F. Brandao, M. Horodecki, N. Ng, J. Oppenheim, S. Wehner, *Proc. Natl. Acad. Sci. USA* **2015**, *112*, 3275.

[40] P. Swiklinski, M. Studzinski, M. Horodecki, J. Oppenheim, *Phys. Rev. Lett.* **2015**, *115*, 210403.

[41] S. Kolkowitz, A. Safira, A. A. High, R. C. Devlin, S. Choi, Q. P. Unterreithmeier, D. Patterson, A. S. Zibrov, V. E. Manucharyan, H. Park, M. D. Lukin, *Science* **2015**, *347*, 1129.

[42] E. S. Tikhonov, D. V. Shovkun, D. Ercolani, F. Rossella, M. Rocci, L. Sorba, S. Roddaro, V. S. Khrapai, *Sci. Rep.* **2016**, *6*, 30621.

[43] Q. Weng, S. Komiyama, Z. An, L. Yang, P. Chen, S.-A. Biehs, Y. Kajihara, W. Lu, *Science* **2018**, *360*, 775.

[44] M. Mintchev, P. Sorba, *J. Phys. A* **2013**, *46*, 095006.

[45] A. Bastianello, L. Piroli, P. Calabrese, *Phys. Rev. Lett.* **2018**, *120*, 190601.